Residual Bouguer satellite gravity anomalies reveal basement grain and structural elements of the Vøring Margin, off Norway

Christian Berndt

Berndt, C.: Residual Bouguer satellite gravity anomalies reveal basement grain and structural elements of the Vøring Margin, off Norway. *Norsk Geologisk Tidsskrift*, Vol. 82, pp. 31–36. Trondheim 2002. ISSN 029-196X.

Free-air gravity data from satellite altimetry and ship-track derived bathymetry data are used to calculate a residual Bouguer gravity anomaly map for the mid-Norwegian Margin. The anomalies were corrected for a density difference between basin sediments and water of 1400 kg m-3 and filtered for wavelengths between 10 and 190 km. A comparison of seismic and magnetic information about the crustal structure corroborates previously identified structural elements and reveals some additional complexity in the margin structure. The strongest negative anomalies relate to the Hel Graben and the Rås Basin indicating that these synclines are deep sedimentary basins. The strongest positive anomalies occur on the Sandflesa High, and the Utgard High and on two segments of the Gjallar Ridge. They relate to metamorphic core complexes and/or basement highs. The gravity anomalies show two regional strike directions, which are presumably associated with Tertiary extension and older weakness zones in the basement. Within the investigated wavelength, residual Bouguer gravity anomaly maps derived from satellite altimetry and ship-track bathymetry are as suitable for investigating regional trends as maps derived from ship-track gravity measurements. Thus, these residual gravity maps provide a powerful aid for seismic interpretation of deep crustal structures.

Christian Berndt, Department of Geology, University of Tromsø, Dramsveien 201, NO-9037 Tromsø, Norway.

Introduction

The Vøring Margin offshore Norway is a current exploration frontier. Therefore, there is a demand for knowledge about its crustal architecture and evolution which has led to both wide-angle seismic studies (Mutter et al., 1984; Eldholm & Mutter, 1986; Planke et al. 1991; Mjelde et al. 1997; Mjelde et al. 2001), and potential field studies (Doré & Lundin 1996; Doré et al. 1997; Olesen et al. 1997; Fichler et al. 1999). Although seismic studies provide more detail and smaller errors along crustal transects, potential field studies have a higher lateral resolution.

The Norwegian Margin was formed by prolonged extension primarily during Jurassic/Early Cretaceous and Late Cretaceous/Early Tertiary times, with final continental breakup in the Early Eocene (Skogseid et al. 2000). The extension was located within the Caledonian collision zone. It is suggested that lithospheric weakness zones date back to the Caledonian orogeny (Brekke & Riis 1987), and later extension focused on these weakness zones. Whereas the early rifting episodes affected a wide area partly including the Trøndelag Platform, Late Cretaceous/Early Tertiary rifting was confined to the outer margin (Doré et al. 1999; Skogseid et al. 2000).

A high density of water depth measurements exists for the Vøring Plateau offshore Norway (Fig. 1). This study uses these measurements to calculate the residual Bouguer gravity anomalies for the sedimentary Vøring Basin from satellite altimetry-derived free-air gravity anomalies, by conducting a 3-D Bouguer correction and applying spatial frequency filters.

The first objective of this study is to provide additional constraints on the predominant strike direction and location of the structural elements of the Vøring Margin. The results of this study are an improvement compared to earlier work based on satellite data because it takes into account the three-dimensional effect of the water layer, it uses a denser line coverage and it uses a well-defined wavelength window.

The second objective is to provide a new residual gravity map that can aid seismic interpretation of the Vøring Margin. The usefulness of such maps for studying deep crustal structures has been shown by earlier comparisons between gravity maps derived from ship track data, and satellite data residual gravity maps (Fichler et al. 1997).

Gravity Processing

As parts of the free-air gravity anomalies are caused by bathymetry due to the gravitational force of the water layer, work to constrain the deep crustal structure from regional gravity measurements should compensate for

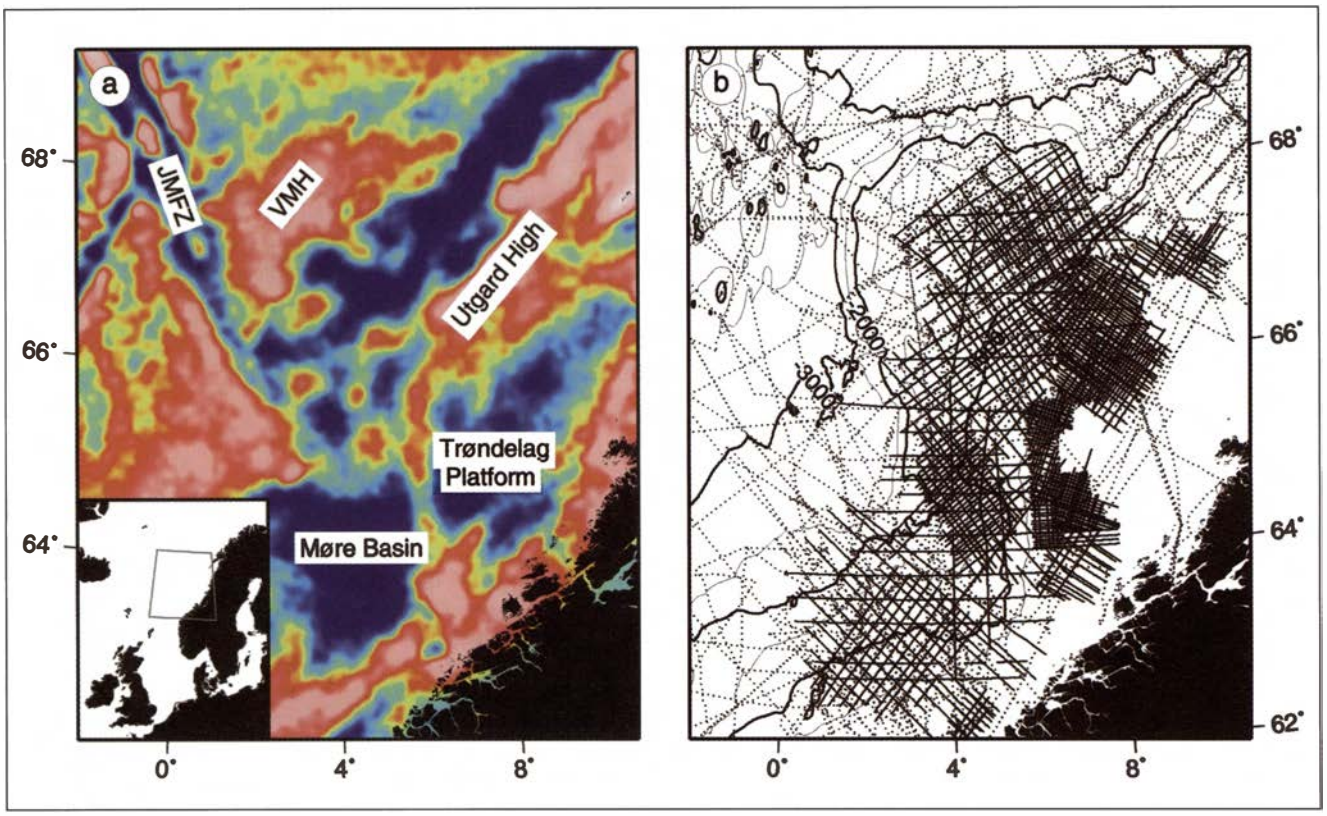

Figure 1. Data used in this study: (a) free-air gravity anomaly and (b) bathymetry contours with corresponding ship-tracks. VMH, Vøring Marginal High; JMFZ, Jan Mayen Fracture Zone.

the effect of the water layer. The traditional method to correct for water depth is the Bouguer correction, which is based on a horizontal slab of infinite extension (Dobrin & Savit, 1988). However, this method is not exact enough in areas such as the one under investigation where there are large variations in water depth. Consequently, a full 3-D approach had to be used in this study. The effect of the water layer is estimated and subtracted from the satellite altimetry-derived free-air gravity anomaly (Sandwell & Smith 1997). The correction is calculated from the bathymetry and for a range of density differences at the seafloor $\Delta\rho$ using the Fourier Transform-based method by Parker (1972) and Luis et al. (1998). A range of $\Delta\rho$ values from 100 to 2700 kg m^{-3} is tested in order to find a $\Delta\rho$ that best reflects the density difference between the water layer and the sediments underneath. Resulting gravity anomalies are shown for different $\Delta\rho$ for one transect in Fig. 2.

The average sediment density is dependent on the thickness of sediments for which the average is taken, i.e. $\Delta\rho$ is higher for deep basins than shallow ones. Thus, even though there is no 'correct' density for the entire study area, a suitable $\Delta\rho$ has to be chosen. A means to do this is Nettleton's method (Nettleton, 1976). It postulates that for the best $\Delta\rho$ the correlation between topography and calculated gravity anomaly is smallest. Comparing gravity maps for different $\Delta\rho$ with the bathymetry it is qualitatively estimated that gravity maps for $\Delta\rho$ = 1400 kg m^{-3} (2400 kg m^{-3} for sediments - 1000 kg m^{-3} for water) fulfil this requirement best. Such a sediment density agrees well with previously reported densities for the Vøring Basin sediments (Skogseid et al. 1992). However, the value is too low for the breakup volcanic rocks. Consequently, the resulting map should not be used for interpretation of the outer Vøring Margin.

The second variable in the gravity correction is the bathymetry. This study uses bathymetry derived from soundings on research vessels (stippled profiles in Fig. 1b) and water depths derived from seafloor picks from multichannel seismic data (solid profiles in Fig. 1b). A water velocity of 1480 m s^{-1} is used to calculate water depth from the measured two-way travel time to the seafloor. The resulting bathymetry grid is more detailed than previous maps for the study area (Perry 1986; Sandwell & Smith 1997), but generally shows a close match. However, the resolution and hence the reliability of the resulting map decreases rapidly west of the Vøring Plateau and close to shore where the available data coverage is sparse (Fig. 1b).

The different wavelength ranges of the gravity signal correspond to different depths of the density variations that cause the gravity signal. Generally, the short wavelength component of the gravity signal is entirely due to shallow density variations, whereas longer wavelengths in the gravity anomaly can be caused by shallow and deep variations. Furthermore, laterally extensive density variations will be isostatically compensated. The wavelength at which the compensation takes place depends

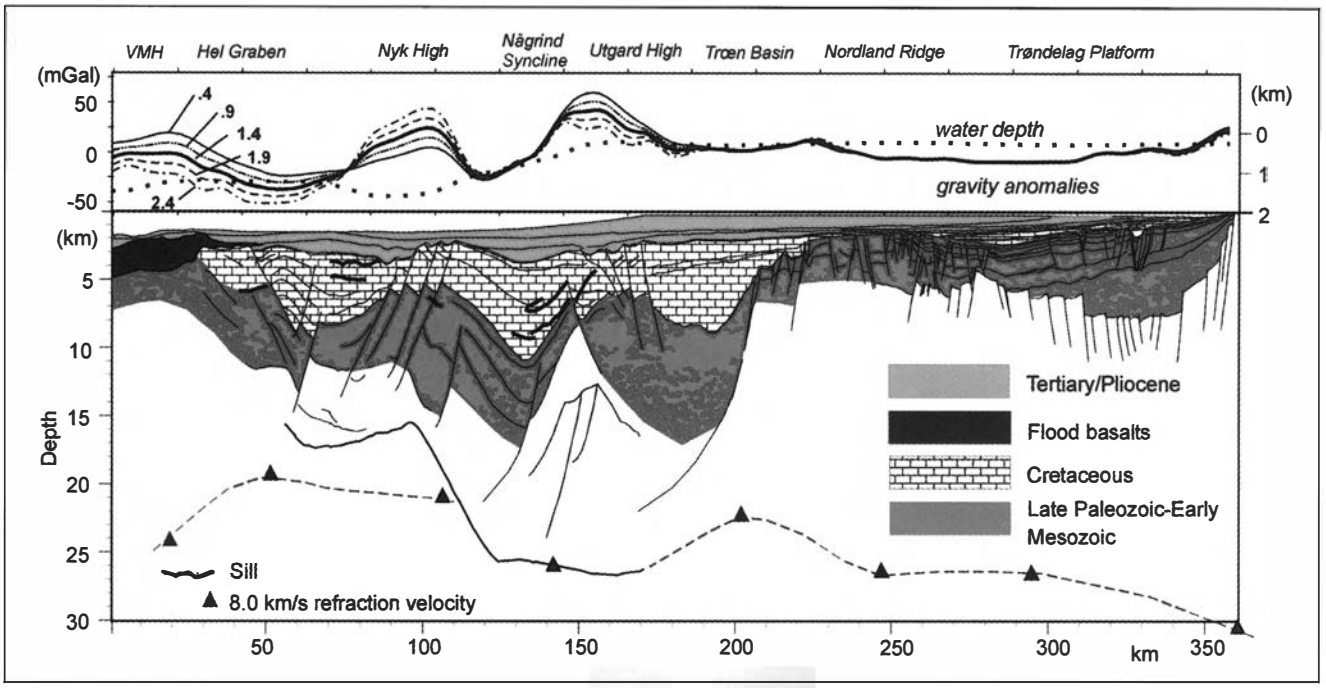

Figure 2. Filtered Bouguer gravity anomalies (top) along a crustal transect (after Skogseid et al., 2000 updated with new constraints on the depth of the Base Cretaceous), location in Fig. 4. Small numbers at the gravity anomaly curves indicate different Δρ values in 1000 kg m⁻³ used for the correction. With Δρ 1400 kg m⁻³ and a spatial filter between 10 and 190 km the solid, bold curve corresponds to the processing used for Fig. 4. VMH, Vøring Marginal High.

on the lithospheric strength (Watts et al. 1985). Assuming that the shallow density variations are not significant compared to deep density variations, it should be possible to design spatial frequency filters that can enhance the signal of mid- and lower-crustal density variations. The assumption is justified because the shallow sedimentary basin fill is far more evenly distributed than the deep basement structures.

A filter is applied for wavelengths shorter than 10 km in order to attenuate noise from erroneous ship-track measurements. Also, the satellite-derived gravity data are filtered at these wavelengths and contain no usable information (Sandwell & Smith 1997 and Fig. 3). High-pass filters are tested for the range between 70 and 360 km in steps of 10 km. The resulting residual gravity map for wavelengths between 10 and 120-150 km shows little lateral continuity with the highs and lows being evenly distributed. Only some prominent features such as the Jan Mayen Fracture Zone are readily distinguished. For wavelengths longer than 150 km a number of pronounced residual gravity anomalies result. These anomalies are strong and vary little until the upper filter wavelength exceeds 340 km. At wavelengths greater than this the residual gravity anomaly becomes similar to the unfiltered, water layer corrected gravity anomaly map as the filter length approaches the dimension of the filtered grid, i.e. approximately 500 by 800 km. To preserve detail in the final residual Bouguer gravity anomaly map (Fig. 4) a high-pass filter with an upper wavelength of 190 km was chosen. The low-pass filter is cosine tapered from 8 to 10 km and the high-pass filter is cosine tapered from 190 to 200 km.

Sensitivity of the method

A comparison of the residual gravity map for the Lofoten Margin derived from ship-track gravity data and the residual Bouguer gravity map derived in this study (Fig. 5) shows a close match. High gravity gradients at the SE flank of the Sandflesa High, which Olesen et al. (1997) interpreted to be caused by a fault zone, are visible in the residual gravity map presented in this study. Small discrepancies, such as the shape of the northern termination of the Utgard High fall within the uncertainties

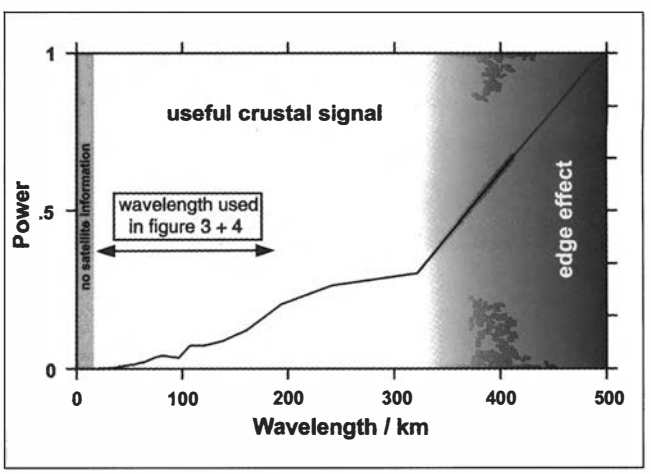

Figure 3. Normalized power spectrum of the free-air gravity anomalies. To obtain high resolution only the frequency component with wavelength between 10 and 190 km is used for the residual gravity map, but maps for filters up to 380 km wavelength yield similar results.

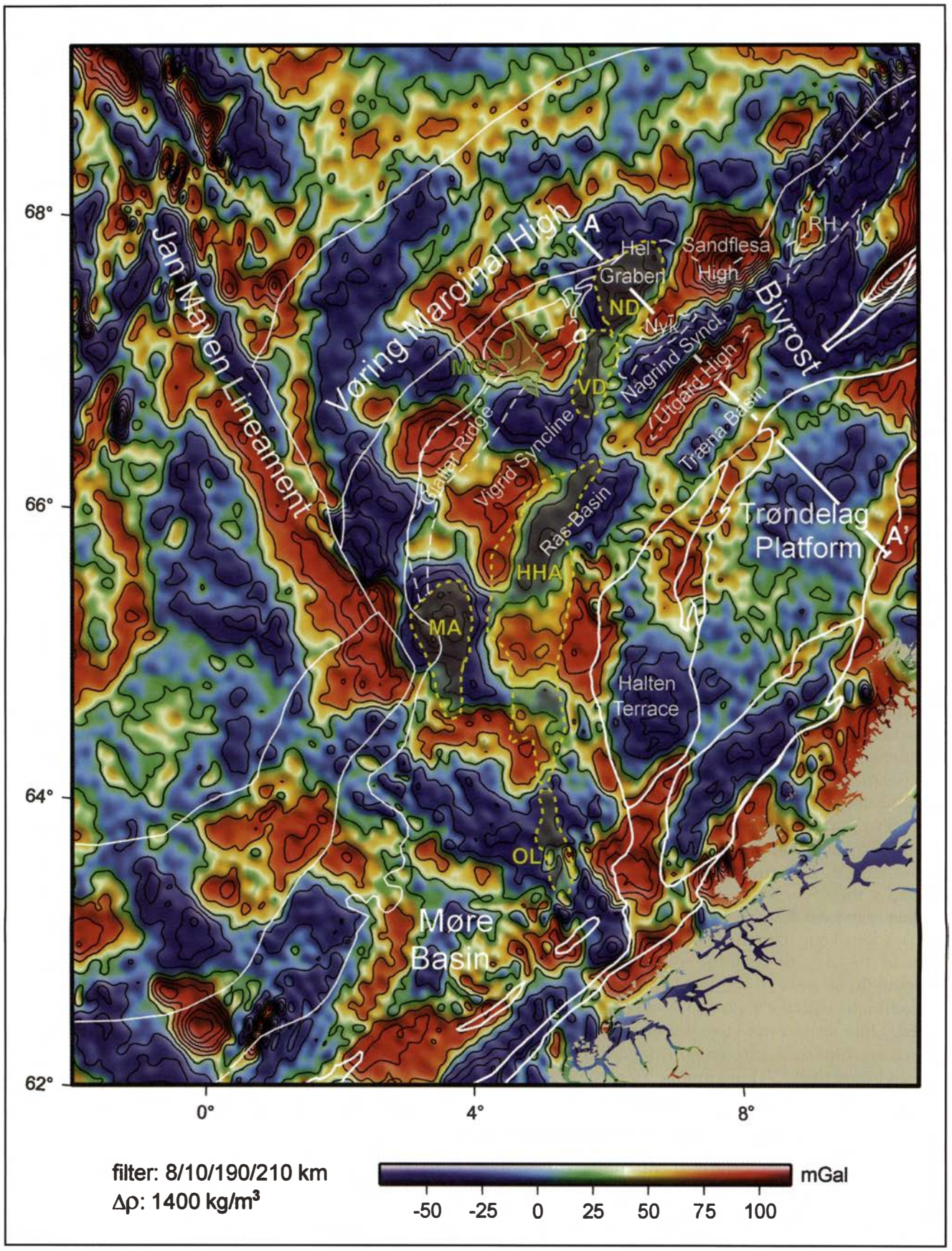

Figure 4. Residual Bouguer gravity map for the Vøring Margin. Structural elements (after Blystad et al., 1995): Tertiary dome structures in red: HHA, Helland-Hansen Arc; VD, Vema Dome; ND, Naglfar Dome; OL, Ormen Lange Dome; MA, Modgunn Arch; other structural elements in white: RH, Røst High; Nyk, Nyk High; Bivrost, Bivrost Lineament. Minimum extent of metamorphic core complex, MCC (after Ren et al., 1998) in green. A-A': Transect shown in Fig. 2.

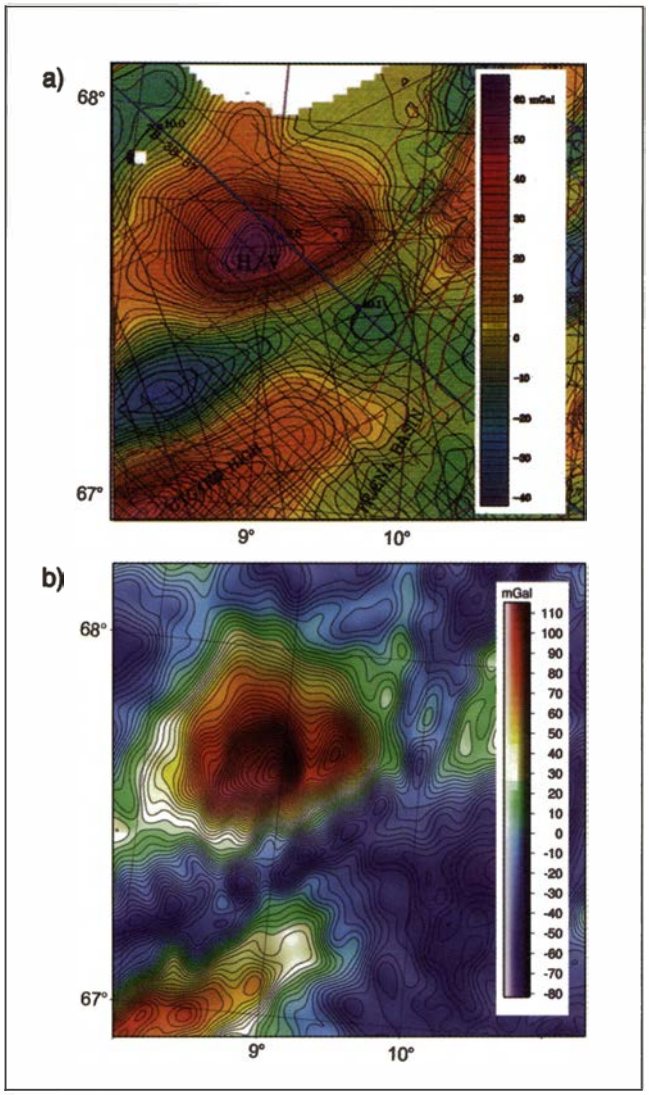

Figure 5. Residual gravity anomaly for the Sandflesa High derived a) from ship-track gravity measurements (Olesen et al., 1997) and b) from satellite altimetry (this study). Note, that absolute values are different, because of different Bouguer gravity corrections and the filters applied.

of both methods. Some short wavelength undulations in the satellite derived gravity data are possibly the result of cross-over errors at satellite track interceptions (Sandwell & Smith, 1997). The match indicates that residual gravity anomalies derived from satellite data are as suited for regional interpretations as residual gravity anomalies derived from ship-track data provided that means of checking the regional water depth exist and are used in the calculation. Generally, ship-track gravity measurements contain a higher frequency content than satellite derived gravity data and must be used for forward gravity modelling. However, this additional information is lost during lateral interpolation between ship-tracks when a regional gravity map is generated. The amount of high-frequency information which can be conserved in a regional map depends on the spacing between individual ship-tracks, but unless the distance between ship-tracks is less than 5 to 10 km the loss of information cancels the difference between the satellite and ship-track gravity data.

The residual gravity anomalies correlate with the main structural elements of the Vøring Basin mapped by seismic data (Fig. 4 and Blystad et al. 1995). The best examples are the extent of the metamorphic core complex at the northern termination of the Gjallar Ridge (Ren et al. 1998) and the extent of the Utgard High (Blystad et al. 1995) which both correlate to positive residual gravity anomalies. The Hel Graben and the Rås Basin match are pronounced negative anomalies.

In fact, the Hel Graben is associated with the strongest negative investigated residual gravity anomaly in the study area. The strongest positive residual gravity anomaly along the margin is the Sandflesa High, named by Olesen et al. (1997), who concluded from magnetic and gravity modelling that it corresponds to a basement high with a top at approximately 6 km. The match between the positive residual gravity anomalies and the basement highs of the Sandflesa High and the Gjallar Ridge, at 6 km (Olesen et al. 1997) and 9 km (Ren et al., 1998) respectively, indicates that the large residual gravity anomalies are caused by intra-crustal density anomalies at this depth or deeper, for example, a contrast between sedimentary basin fill and crystalline basement. This implies that the assumption of little lateral density variability within the shallower parts of the basin holds. However, the residual gravity map can neither resolve changes in absolute depth nor distinguish between different sources of density variation such as basement highs or metamorphic core complexes. Nevertheless, the good match between density differences inferred from independent techniques and the calculated anomalies suggests that it is possible to use the residual gravity map to study large-scale variations.

Results

The residual gravity map indicates a main SW-NE structural strike direction parallel to the Tertiary breakup-axis. The Utgard High, the Någrind Syncline, the Træna Basin, the Rås Basin, and anomalies within the Møre Basin strike in this direction, whereas the Jan Mayen Fracture Zone is oriented perpendicular to this first axis (Doré & Lundin 1996).

The new residual gravity map also corroborates a weaker, second trend of strike in NS direction. The Tertiary domes, such as the Helland-Hansen Arc, the Naglfar Dome, the Vema Dome and the Ormen Lange Dome line up along this trend, and they are generally associated with negative residual gravity anomalies. This indicates deep basins underneath the domes. Doré and Lundin (1996) suggested that the NS striking second trend corresponds to older weakness zones within the basement that were preferentially reactivated during Mesozoic and Early Cenozoic rifting.

The residual gravity anomaly confirms most structural elements that are included in the compilation by Blystad et al. (1995). It reveals, however, some complexities that the literature has paid little attention to: (a) The Gjallar Ridge in the western Vøring Basin includes three positive and two negative residual gravity anomalies. The northernmost is located where Ren et al. (1998) identified a metamorphic core complex. This might suggest that also the other two positive anomalies on the Gjallar Ridge result from similar features. (b) The Sandflesa High at the boundary between the Vøring and Lofoten-Vesterålen margins shows the highest residual gravity anomalies in the study area and must be an important crustal anomaly that was not included in previous compilations of the structural elements. (c) The Tertiary dome structures at shallow depth are associated with negative residual gravity anomalies indicating that they developed in thick sedimentary successions. This supports their interpretation as inversion structures (Doré & Lundin 1996; Fichler et al. 1999). However, the Helland-Hansen Arc also covers areas with broad residual gravity highs indicating a deep intra-basement anomaly.

Acknowledgements. - I thank RWE-DEA Norge AS for providing the bathymetry information and Joaquim Luis for making his grav3d program publicly available. Jakob Skogseid provided an update of his crustal transect on the northern Vøring Plateau. Asbjørn Breivik and Michel Heeremans made helpful comments on earlier versions of the manuscript and Christine Fichler, Jakob Skogseid and an anonymous reviewer provided useful insight. GMT (Wessel & Smith 1991) was used extensively for data preparation.

References

Blystad, P., Brekke, H., Færseth, R.B., Larsen, B.T., Skogseid, J. & Tørudbakken, B. 1995: Structural elements of the Norwegian continental shelf II: The Norwegian Sea. Norwegian Petroleum. Directorate.

Brekke, H. & Riis, F. 1987: Tectonics and basin evolution of the Norwegian shelf between 62°N and 72°N. *Norsk Geologisk Tidsskrift 67*, 295-322.

Dobrin, M.B. & Savit, C.H. 1988: *Introduction to geophysical prospecting.* McGraw-Hill, New York.

Doré, A., Lundin, E., Birkeland, Ø., Eliassen, P., & Jensen, L. 1997: The NE Atlantic margin: implications of late Mesozoic and Cenozoic events for hydrocarbon prospectivity. *Petroleum Geosciences 3*, 117-131.

Doré, A.G. & Lundin, E.R. 1996: Cenozoic compressional structures on the NE Atlantic margin: nature, origin and potential significance for hydrocarbon exploration. *Petroleum Geosciences 2*, 299-311.

Doré, A.G., Lundin, E.R., Jensen, L.N., Birkeland, Ø., Eliassen, P.E., & Fichler, C. 1999: Principal tectonic events in the evolution of the northwest European Atlantic region. *In* Fleet, A.J. & Boldy, S.A. (eds.): *Petroleum Geology of Northwest Europe: Proceedings of the 5th conference.* Geological Society of London, 41-61.

Eldholm, O. & Mutter, J. C. 1986: Basin structure on the Norwegian margin from analysis of digitally recorded sonobuoys. *Journal of Geophysical Research 91 B3*, 3763-3783.

Fichler, C., Rundhovde, E., Johansen, S. & Sæther, B.M. 1997: Barents Sea tectonic structures visualized by ERS1 satellite gravity data with indications of an offshore Baikalian trend. *First Break 15 (11)*, 355-363.

Fichler, C., Rundhovde, E., Olesen, O., Sæther, B.M., Rueslåtten, H., Lundin, E. & Doré, A.G. 1999: Regional tectonic interpretation of image enhanced gravity and magnetic data covering the mid-Norwegian shelf and adjacent mainland. *Tectonophysics 306*, 183-197.

Luis, J.F., Miranda, J.M., Galdeano, A. & Patriat, P. 1998: Constraints on the structure of the Azores Spreading Center from gravity data. *Marine Geophysical Research 20*, 157-170.

Mjelde, R., Digranes, P., Van Schaack, M., Shimamura, H., Shiobara, H., Kodaira, S., Næss, O., Sørenes, N. & Vågnes, E. 2001: Crustal structure of the outer Vøring Plateau NE Atlantic, from wide-angle seismic and gravity data. *Journal of Geophysical Research 106 (B7)*, 6769-6791.

Mjelde, R., Kodaira, S., Shimamura, H., Kanazawa, T., Shiobara, H., Berg, E.W. & Riise, O. 1997: Crustal structure of the central part of the Vøring Basin, mid-Norway margin, from ocean bottom seismographs. *Tectonophysics 277*, 235-257.

Mutter, J.C., Talwani, M. & Stoffa, P.L. 1984: Evidence for thick oceanic crust adjacent to the Norwegian margin. *Journal of Geophysical Research 89 (B1)*, 483-502

Nettleton, L.L. 1976: *Gravity and Magnetics in Oil Prospecting.* McGraw Hill, New York.

Olesen, O., Torsvik, T.H., Tveten, E., Zwaan, K.B., Løseth, H. & Henningsen, T. 1997: Basement structure of the continent margin in the Lofoten-Lopphavet area, northern Norway: constraints from potential field data, on-land structural mapping and paleomagnetic data. *Norsk Geologisk Tidsskrift 77*, 15-30.

Parker, R.L. 1972: The rapid calculation of potential anomalies. *Geophysical Journal of the Royal Astronomical Society 31*, 447-455.

Perry, R.K. 1986: Bathymetry. *In* Hurdle, B. (ed.): *The Nordic seas*, 211-235. Springer Verlag, New York.

Planke, S., Skogseid, J. & Eldholm, O. 1991: Crustal structure off Norway, 62° to 70° north. *Tectonophysics 189*, 91-107.

Ren, S., Skogseid, J. & Eldholm, O. 1998: Late Cretaceous-Paleocene extension on the Vøring volcanic margin. *Marine Geophysical Research 20*, 343-369.

Sandwell, D.T. & Smith, W. H.F. 1997: Marine gravity anomaly from Geosat and ERS 1 satellite altimetry. *Journal of Geophysical Research 102 (B5)*, 10,039-10,054.

Skogseid, J., Pedersen, T. & Larsen, B.T. 1992: Vøring basin: subsidence and tectonic evolution. *In* Larsen, R.M., Brekke, H., Larsen, B.T., & Talleraas, E. (eds.): Structural and Tectonic Modelling and its Application to Petroleum Geology. *Norwegian Petroleum Society Special Publication 1*, 55-82.

Skogseid, J., Planke, S., Faleide, J.I., Pedersen, T., Eldholm, O. & Neverdal, F. 2000: Atlantic continental rifting and volcanic margin formation. *In* Nøttvedt, A. (ed.): Dynamics of the Norwegian Margin. *Geological Society of London Special Publication 167*, 295-326.

Watts, A.B., ten Brink, U., Buhl, P. & Brocher, T. 1985: A multi-channel seismic study of lithosphere flexure across the Hawaiian-Emperor seamount chain. *Nature 315*, 105-111.

Wessel, P. & Smith, W.H.F. 1991: Free software helps map and display data. *Eos Transactions of the American Geophysical Union 72*, 441, 445-446.